Comparison of Kinematic Behaviour of a First Generation Obese Dummy and Obese PMHS in Frontal Sled Tests

Hamed Joodaki, Jason Forman, Ali Forghani, Brian Overby, Richard Kent, Jeff Crandall, Breanna Beahlen, Mike Beebe, Ola Bostrom

Abstract The purpose of this study is to evaluate a First Generation Obese Anthropometric test device (FGOA), comparing its kinematic behaviour with two obese Post Mortem Human Surrogates (PMHS) in matching frontal impact sled tests.

The FGOA was built around an existing 50th percentile THOR male crash test dummy's skeletal structure, but with unique flesh and additional mass added to the upper and lower torso and upper legs. Two 29 km/h PMHS tests, two 48 km/h PMHS tests, two 29 km/h dummy tests, and two 48 km/h dummy tests were performed with a sled buck representing the rear seat occupant component of a 2004 mid-sized sedan.

The FGOA and PMHS exhibited similar kinematic characteristics, which have been highlighted previously as potentially challenging for restraint systems design. Most notably, both the PMHS and dummy exhibited substantial forward motion of lower body and subsequent backwards rotation of the torso, affected by limited engagement of the lap-belt with the pelvis. Although some differences suggest that further refinement may be warranted, the similarities suggest that this dummy may prove useful as a research tool to begin investigating the challenges of, and potential strategies for, the safe restraint of obese occupants.

Keywords obese dummy, obesity, frontal impact, biofidelity, dummy development.

I. Introduction

Body Mass Index (BMI), also known as Quetelet's Index, which is individual's mass divided by square of height (kg/m^2), is a commonly used measure of obesity in the adult population. According to the World Health Organization (WHO), people with BMI of 30 kg/m^2 or higher are considered to be obese [1].

Obesity has increased during the past three decades in the USA. Between the periods of 1988–1989 and 2003–2004, the waist circumference and abdominal obesity among US adults have increased continuously [2]. Average BMI increased by 0.37% per year in both male and female US adults from 1988 to 2010 [3]. In 2009–2010, over 78 million US adults and about 12.5 million US children and adolescents were classed as obese [4]. In 2011–2012, 34.9% of US adults age 20 years or older had BMI of more than 30 kg/m^2 [5].

Many studies have reported increased risk of mortality for obese patients suffering blunt trauma. In a study of 351 hospital patients with blunt trauma, Choban et al. [6] observed significantly higher mortality and complication rates for patients with BMI greater than 31 kg/m^2. Similarly, Neville et al. [7] compared mortality rates of obese and non-obese patients with blunt trauma and reported obesity as an independent predictor of mortality following severe blunt trauma.

In addition to the general relationship between blunt trauma mortality and obesity, there is also an increased risk of death in motor vehicle crashes among obese occupants [8]. Mock et al. [9] studied 36,206 crash involved automotive occupants and, after adjustment for potentially confounding variables, found a significant relationship between an occupant's BMI and mortality. In a study of 155,584 drivers who died in severe motor vehicle crashes, Jehle et al. [10] observed an increased risk of death for drivers with BMI>35 kg/m^2 and BMI<18.5 kg/m^2, and a decreased mortality risk in drivers with 25 kg/m^2 <BMI<30 kg/m^2. Rice et al [11] found that drivers with 35 kg/m^2 <BMI<39.9 kg/m^2 and BMI>40 kg/m^2 are 48% and 78%, respectively, more likely to

H. Joodaki is a research assistant at Center for Applied Biomechanics (CAB), USA, and a graduate student in Mechanical Engineering Department of University of Virginia (UVA), USA. J. Forman is principal scientist, A. Forghani is research specialist, B. Overby is research engineer and lab specialist in CAB, USA. R. Kent is Professor in Mechanical Engineering Department of UVA, USA, and Deputy Director of CAB, USA. J. Crandall is Professor in Mechanical Engineering Department of UVA, USA, and the director of CAB, USA. B. Beahlen is mechanical engineer and M. Beebe is chief technology officer in Humanetics Innovative Solutions Incorporation, USA. O. Bostrom is Integrated Safety Director of Autoliv Research, Sweden.

have a fatal injury than normal BMI drivers.

Obesity is also likely to have an effect on acute injury risk. Arbabi et al. [12] reported that there is an increased risk of lower extremity injuries, in addition to an increased risk of mortality, for obese occupants. Cormier [13] observed that obese occupants had a higher risk of thoracic injury compared to lean occupants.

Potential mechanisms for increased injury risk have also been observed experimentally. Kent et al. [14] and Forman et al. [15] compared mid-sized and obese post mortem human surrogate (PMHS) occupants' kinematics in simulated frontal crashes and observed that, generally, obese occupants experienced greater maximum forward displacement within the occupant compartment. They reported larger hip excursion (defined as the forward displacement relative to the vehicle interior) as the primary difference between mid-size and obese cadavers, due to limited engagement of the pelvis by the lap-belt. This increase in forward motion of the pelvis also resulted in backwards rotation of the torso, applying a greater portion of the shoulder-belt load to the more vulnerable lower chest [15].

Obese occupants present a significant challenge for current restraint systems. Obesity is associated with the lap-belt being further forward and higher relative to the pelvis [16], limiting the ability of the lap-belt to properly engage the pelvis when in a frontal collision. The increased depth of subcutaneous tissue, combined with increased body mass, may dramatically increase the amount of forward excursion observed before the restraint system arrests the occupant's motion. Forman et al. [15] observed that obese subjects exhibited fundamentally different kinematics compared to mid-size subjects, interacting with the seat and belt restraint system in a manner that could not be anticipated through observations with mid-size male dummies. The improvement of obese occupant safety requires a tool capable of interacting with restraint systems and vehicle interiors in a manner that replicates the challenges posed by obese occupants.

In this effort, a first generation of obese anthropometric test device (FGOA) has been developed. The objective of this study is to present characteristics of this FGOA and to perform a preliminary evaluation of its biofidelity by comparing the kinematic behaviours of this dummy with those of two obese PMHS in frontal collisions under matched testing conditions.

II. METHODS

ATD Development

The FGOA is built on an existing platform of the THOR-FT 50th percentile male anthropometric test device (ATD, Fig. 1). The conversion to the obese ATD was accomplished through a flesh jacket representing the superficial tissue of an obese male. The flesh jacket consisted of chest, pelvis and upper thigh fleshes. The chest jacket was made from silicone and the thigh and pelvis fleshes were made from a polyurethane mixture poured around foam. They were constructed from these molded materials to allow the flesh to be pliable enough so that the dummy buttock and thighs would fit and conform into the seat. The legs and arms were ballasted to meet their target masses (Table I).

To facilitate comparison, the external geometry and overall body mass of the current prototype of the FGOA jacket is based specifically on the anthropometry of one of the PMHS previously tested in frontal impact tests (number 404, BMI 35 kg/m^2, Table II).

The internal skeletal dimensions of that subject (e.g. the internal diameter of the rib cage) were similar to those of a 50th percentile male PMHS [15]. Thus, the majority of the difference in the mass and exterior dimensions between this particular obese subject and a nominal 50th percentile male occurred as a result of increased superficial tissue and abdominal fat. For the altered components, the mass distribution was chosen roughly based on the original mass distribution of the THOR dummy (Table I).

Fig. 1. Completed obese ATD prototype.

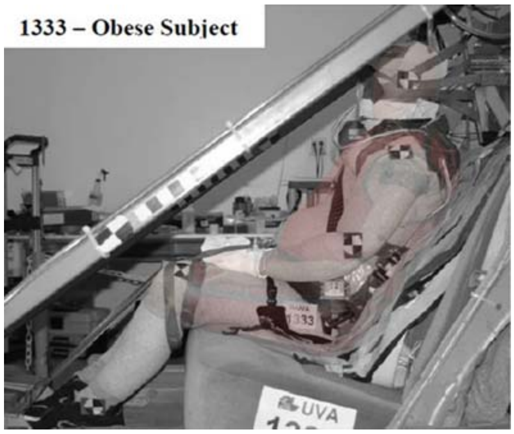

Fig. 2. Overlay of obese ATD with PMHS #404.

TABLE I
BODY MASS DISTRIBUTION

Segment	Hybrid III (kg, %)	THOR (kg, %)	FGOA (kg, %)
Head	4.53 (5.8%)	4.62 (6.1%)	4.62(3.7%)
Neck	1.54 (1.9%)	1.65 (2.2%)	1.65(1.3%)
Upper Torso	17.19 (22.1%)	13.42 (17.9%)	22.22(17.9%)
Lower Torso	23.04 (29.7%)	28.25 (37.7%)	50.80(41.0%)
Upper Arm (each)	1.99 (2.5%)	1.99 (2.6%)	3.28(2.6%)
Lower Arm + Hand (each)	2.26 (2.9%)	2.26 (3.0%)	3.74(3.0%)
Upper leg (each)	5.98 (7.6%)	4.45 (5.9%)	7.34(5.9%)
Lower leg + feet (each)	5.44 (7.0%)	4.75 (6.3%)	7.89(6.3%)
Total mass	77.70	74.91	123.79

TABLE II
FGOA VS. PMHS EXTERNAL MEASUREMENTS

	FGOA	PMHS #404	PMHS #400
Mass	123.8	124	151
Stature	175	189	182
Chest Breadth - 4th Rib	42	40	39
Chest Breadth - 8th Rib	41	36	40.5
Chest Depth - 4th Rib	29	23.5	28.3
Chest Depth - 8th Rib	30	25.5	31.5
Hip Breadth	44.5	39.1	40
Chest Circumference - 4th Rib	130	110.7	124
Chest Circumference - 8th Rib	119	114.3	131
Waist Circumference - At Umbilicus	123.5	120	140
Waist Circumference - 8 cm above Umbilicus	120	119.7	136
Waist Circumference - 8 cm below Umbilicus	126	116.9	139.4
Thigh Circumference	65	68.6	74
Shoulder Breadth (Biacromial)	49	43	38.5
Seated Head to Buttock	93.5	98	110

Dimension unit: cm, Mass unit: kg

Once the Obese ATD prototype was complete, the external dimensions were measured and compared to those of the PMHS #404 (Table II). An overlay picture of that PMHS and Obese ATD is shown in Fig. 2. Minor dimensional differences were noticed between the flesh jacket and PMHS.

PMHS Subjects

Two obese PMHS were used, whose characteristics can be found in Table II. They were screened for HIV and hepatitis A, B and C. They were CT-scanned for pre-existing injuries and preserved until preparing for testing by freezing at 0 °C. The subjects' pulmonary and cardiovascular systems were pressurised to a nominal in vivo level (approximately 10 kPa for both) via tracheostomy and Hetastarch blood plasma replacement solution immediately prior to testing. All PMHS handling and test protocols were approved by the University of Virginia Center for Applied Biomechanics Oversight Committee.

Although a portion of results of PMHS tests were published previously [14-15], all of the data have been reanalysed to facilitate comparison to the dummy.

Sled and Information of Tests

The test buck was mounted to a sled system (deceleration sled for the PMHS tests; acceleration sled for the dummy tests), which generated deceleration pulses based on frontal barrier tests of a mid-sized sedan. Tests were performed with nominal changes in velocity (ΔVs) of 29 km/h and 48 km/h. Acceleration plots of the tests are shown in Fig. 3. Buck accelerations were similar in each speed group. Table III provides the test matrix.

TABLE III
TEST MATRIX

Test Number	S0277	S0278	S0279	S0280	1332	1333	1334	1335
Speed (km/h)	29	48	29	48	29	48	29	48
Subject	FGOA	FGOA	FGOA	FGOA	PMHS 404	PMHS 404	PMHS 400	PMHS 400

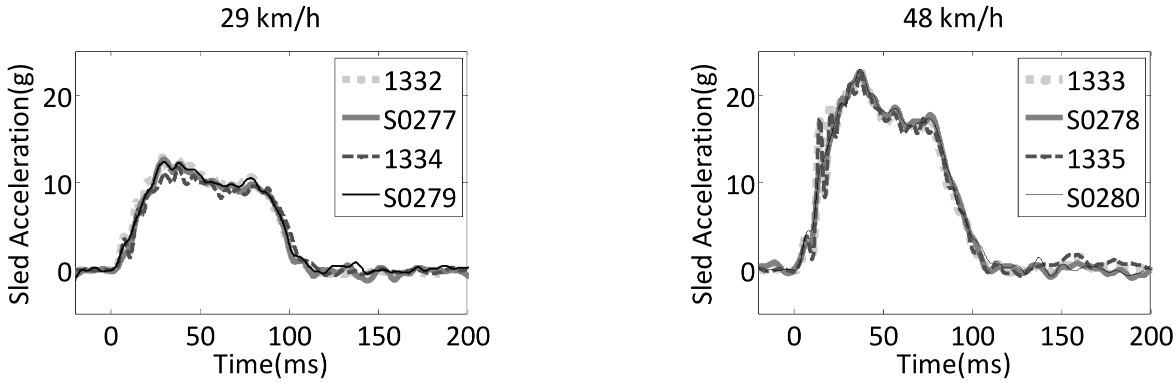

Fig. 3. Sled acceleration of different tests. Buck accelerations were similar in each speed group.

Positioning

The subjects were positioned in the right seating position of a sled buck, representing the rear-seat occupant compartment of a 2004 mid-sized sedan. The initial positioning measurements and the descriptions can be found in Tables IV and V, and in Figs 4 and 5. The front seats of the buck were removed in order to observe the interaction of the subjects with the rear seat and seatbelt without the potentially confounding effects of interaction between the knees and the front seatback. All tests were performed with a three-point belt restraint that included a deck-mounted retractor, a retractor pretensioner and a progressive force-limiter. The first force level of the restraint system was approximately 2.9 kN, and the second force level started from 4.2 kN (see [17]).

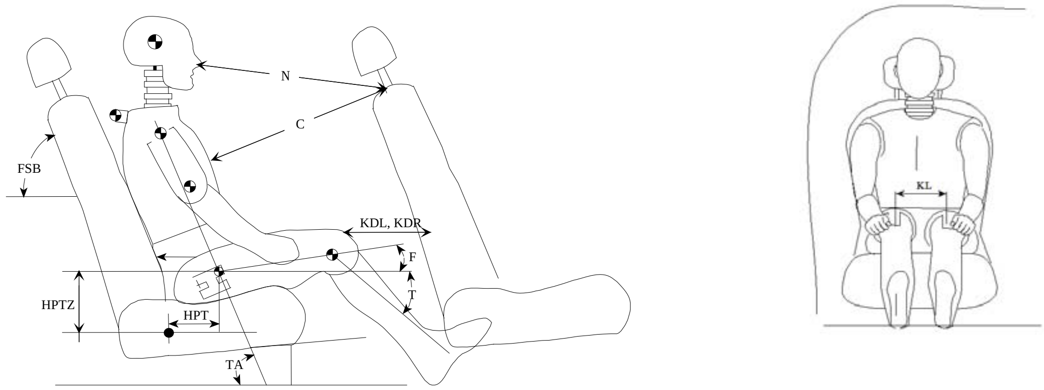

Fig. 4. Description of positioning parameters of Table IV. FSB: Front Seat back angle (from vertical), HPT: H-point longitudinal distance from seat (+ is forward of rear seat), HPTZ: H-point vertical distance from seat (+ is above seat), C: Chest centre line to Front Seat (horizontal distance, to top edge of seat), KL: Lateral distance, right knee centre line to left knee centreline, F: Femur angle (from horizontal), T: Tibia angle (from horizontal), KDL: Left knee to front seat back (closest distance), KDR: Right knee to front seat back (closest distance), N: Nose to front seat back (shortest distance to top edge), TA: Torso angle (angle of line from shoulder to H-point, from horizontal).

TABLE IV
POSITIONING MEASUREMENTS

	Test							
Parameter	1332	1333	1334	1335	S0277	S0278	S0279	S0280
FSB	68	68	68	68	69	68	69	69
HPT	14	22	17	28	20	20	19	21
HPTZ	0	19	nm*	nm	24	25	15	15
C	607	619	587	594	610	615	617	615
KL	295	295	335	350	300	300	300	300
F	16	23	16	19	19	19	19	19
T	51	53	52	58	59	57	59	59
KDL	218	199	178	115	222	224	204	199
KDR	214	192	174	117	202	203	203	198
N	694	717	633	625	670	715	715	716
TA	72	69	75	71	71	68	70	70

All dimensions in millimeters, angles in degrees.
nm*: not measured.

TABLE V
BELT POSITIONING DATA

Label	Unit	1332	1333	1334	1335	S0277	S0278	S0279	S0280
A**	mm	0	0	5	0	42	67	51	55
B	mm	112	108	71	67	60	88	72	71
C	mm	284	286	252	212	E*	298	305	292
D	mm	342	335	303	265	E*	377	385	367
E	deg	41	41	38	41	50	48	44	44
F	deg	-2	2	0	7	5	3	3	1

E*: Error in measurement.

A**: FGOA did not have neck flesh. Hence, A is not comparable between the FGOA and PMHS and it is included simply for future reference.

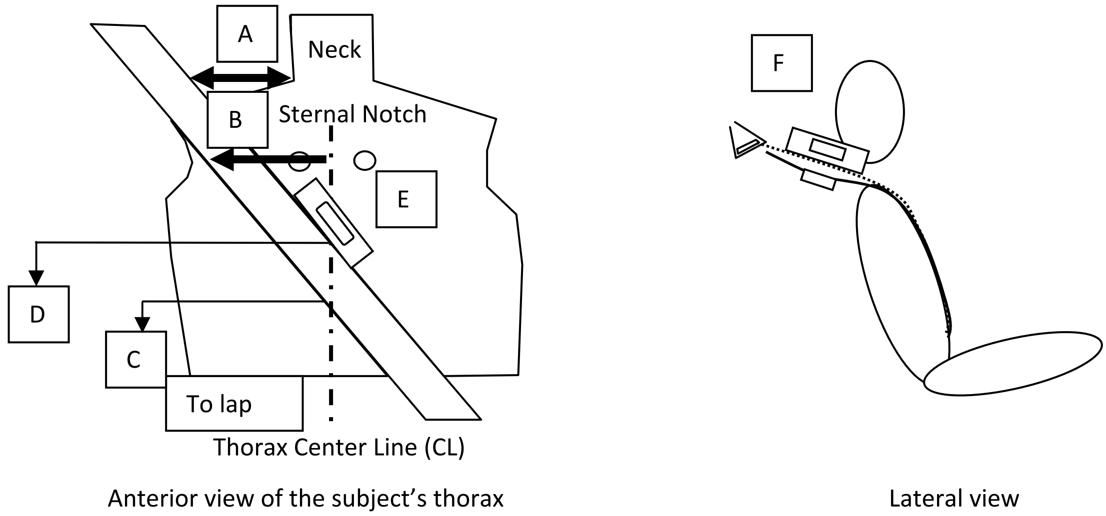

Fig. 5. Description of belt positioning parameters of Table V. A: Lateral neck edge to medial belt edge, B: Lateral belt edge to CL at sternal notch, C: Top of lap plate to lower belt edge on CL, D: Top of lap plate to upper belt edge on CL, E: Angle of belt from horizontal, F: Lateral angle of belt from front edge of retractor to shoulder along tape (straight line).

Video-tracking

High-speed video cameras recorded the tests at a frame rate of 1,000 Hz from offboard passenger side and driver-side views. Target markers were mounted to the subjects' head, shoulder, hip and knee. First, target marker positions were tracked with 1 ms steps, to have their positions in pixel units [19]. Each body part was tracked until its maximum forward motion (maximum displacement in posterior-anterior direction). Interpolation was used for the periods during which targets were covered by vehicle components or other body parts. Using two length reference markers, one for the vehicle target marker plane and another for occupant plane, pixel-to-metre conversion coefficients were defined to convert positions from pixel unit to metre. Tracking a reference point on the vehicle, relative motions of the targets with respect to the buck were determined. Then the processed data were filtered, using the following equation:

$$(X'(t), Y'(t)) = \frac{(X(t-1), Y(t-1)) + 2(X(t), Y(t)) + (X(t+1), Y(t+1))}{4} \quad (1)$$

where *(X'(t),Y'(t))* and *(X(t),Y(t))* are the filtered and unfiltered, respectively, coordinates in time *t*. The origin of the coordinate system was shifted to the initial position of the hip target marker for each test. Moreover, by having shoulder and hip positions at each moment, torso angle (see Fig. 4 for definition) of each test was determined from 0 ms until maximum shoulder excursion time. Since the calculated angles were the angle of line connecting shoulder and hip target marker with –X direction, torso angle results were shifted in order to match the initial torso angles with data of Table IV.

Accelerometers

To record PMHS acceleration, accelerometers were mounted on different locations of body during subject preparation procedure (see [15]). The dummy's accelerations of different body segments were measured using tri-axial accelerometer cubes placed at the head centre of gravity (c.g.), chest c.g. and pelvis. All data were sampled at 10,000 Hz. The following steps were taken to process the data post-test:

- The signals were truncated to include the data between -10 and 200 ms, with 0 ms being the sled acceleration onset.
- The truncated data was then filtered according to the SAE J211 classes.
- The truncated and filtered data was debiased by taking the mean signal value between -10 and 0 ms and subtracting it from the rest of the signal.

III. RESULTS

Data peak summary is presented in Table VI. In tests S0278, a spike (Fig. 6) occurred that may be attributable to looseness in a spine joint, which was tightened in subsequent tests. This spike was observed in the head, pelvis and chest acceleration time-histories. In order to have a logical comparison between acceleration histories of the FGOA and PMHS, this spike was removed. In 48 km/h FGOA tests, other spikes were observed in head acceleration time-histories, which were caused by the hand impact with the head (Fig. 6). In 48 km/h tests, other spikes in the subjects' pelvis acceleration time-histories happened when the subjects travelled off the front edge of the seat. Since these spikes were attributable to acute physical phenomena that were not the focus of this investigation, they are ignored in Table VI (3ms clip used for pelvis) and in choosing Y-limits in Fig. 8.

TABLE VI
SELECTED PEAK DATA

		29km/h Tests				48km/h Tests			
Test Number	Unit	S0277	S0279	1332	1334	S0278	S0280	1333	1335
Subject Type		FGOA	FGOA	PMHS	PMHS	FGOA	FGOA	PMHS	PMHS
Max. Head Acceleration	g	25.5	22.1	21.7	19.7	45.9	47.7	39.4	38.0
Max. Pelvis Acceleration	g	20.1	16.4	20.8	17.8	25.7	22.8	31.7	55.5
Max. Chest/T8 Acceleration*	g	19.8	17.3	22.5	18.8	32.1	37.2	27	30.1
Max. Head Angular Velocity	rad/s	26.8	24.9	18.3	14.4	67.6	60	31.8	25.5
Max. Lower Shoulder-belt Force	kN	3.67	3.36	2.94	2.74	6.88	6.80	6.07	7.16
Max. Upper Shoulder-belt Force	kN	4.35	4.20	4.60	4.38	6.02	5.87	6.33	6.59
Max. Lap-belt Force	kN	5.87	5.49	2.83	4.04	10.38	11.11	8.82	9.35
Max. Head Forward Motion (MHFM)	m	0.43	0.44	0.45	0.46	0.63	0.66	0.62	0.49
Max. Shoulder Forward Motion	m	0.36	0.33	0.33	0.36	0.55	0.58	0.53	0.50
Max. Pelvis Forward Motion	m	0.25	0.21	0.16	0.20	0.48	0.50	0.39	0.46
Max. Knee Forward Motion	m	0.28	0.25	0.16	0.23	0.41	0.48	0.33	0.30

*Chest acceleration for the FGOA and T8 acceleration for the PMHS.

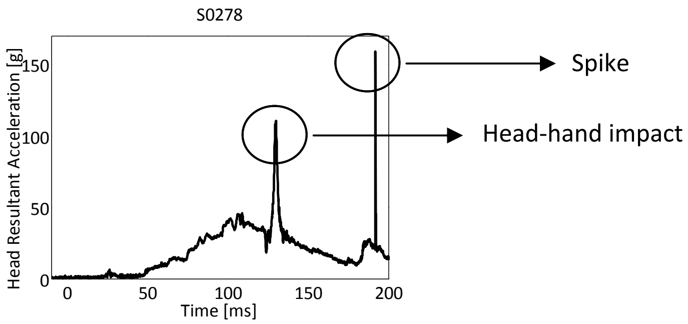

Fig. 6. Illustration of spike seen in resultant head acceleration of test S0278. This spike was removed for calculation of the peak and plot of accelerations for test S0278.

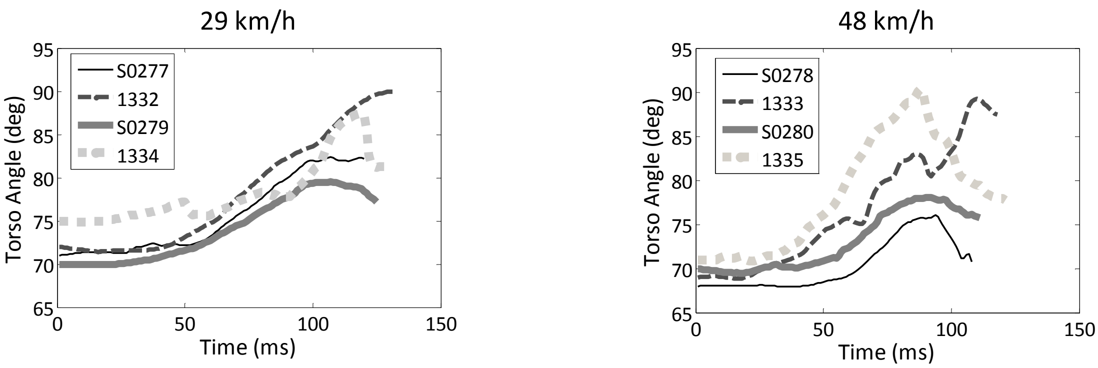

Fig. 7. Calculated torso angle time-histories. *Left*: 29 km/h tests, *right*: 48 km/h tests.

Figure 7 illustrates torso angles for both the FGOA and PMHS groups until maximum shoulder forward motion for all tests. Head, pelvis, chest (for the FGOA) and T8 (for the PMHS) accelerations of all tests are exhibited in Fig. 8. The subjects' head c.g., shoulder, hip and knee motion trajectories are shown in Fig. 9.

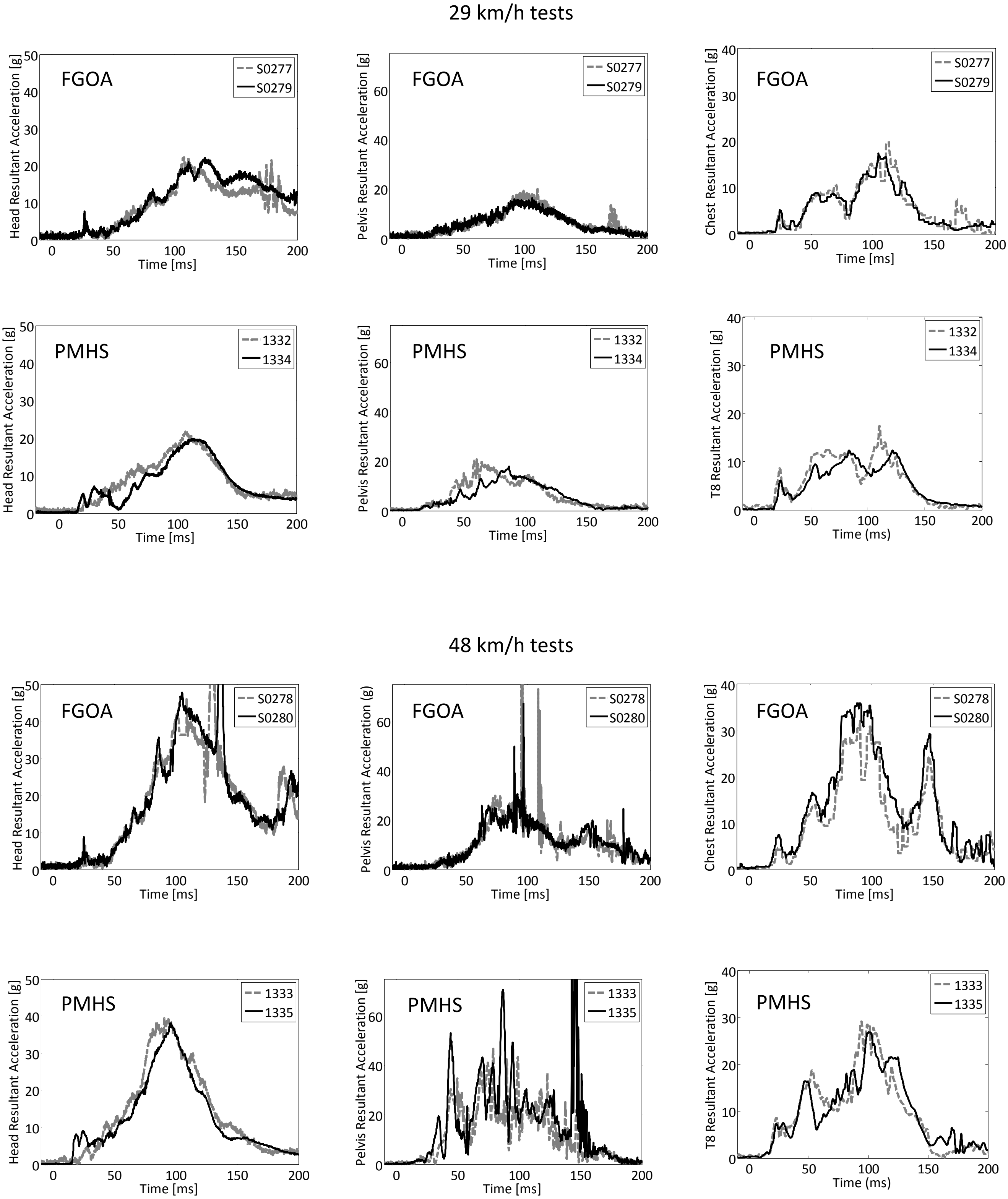

Fig. 8. Accelerarion-time histories of all tests.

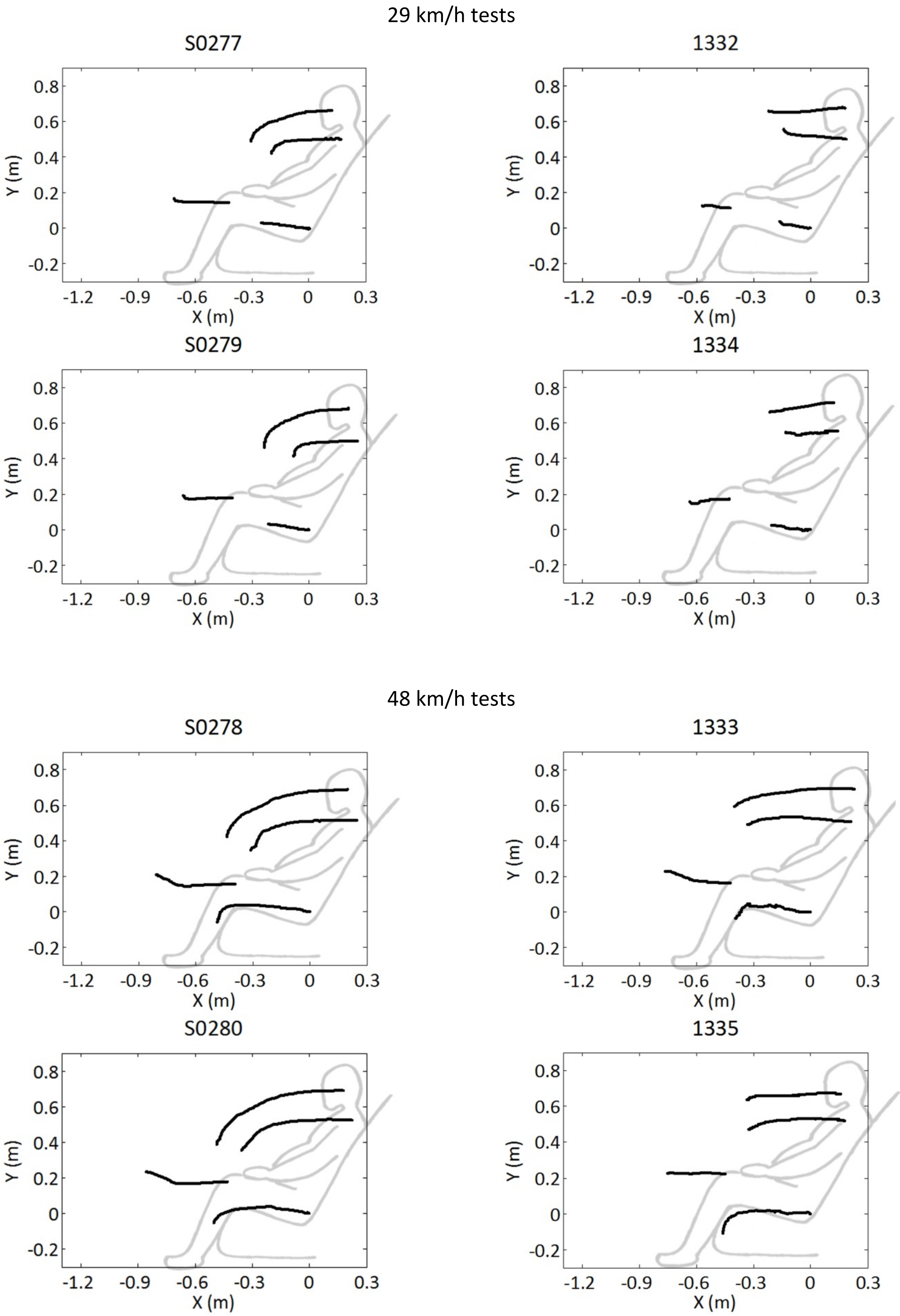

Fig. 9. Head c.g., shoulder, hip and knee trajectories of all tests.

IV. DISCUSSION

ATD Anthropometry

Obesity is categorised into three different classes: class 1: 30 kg/m^2<BMI<35 kg/m^2; class 2: 35 kg/m^2<BMI<40 kg/m^2; and class 3: BMI>40 kg/m^2 [21]. Increased risk of mortality in automobile crashes tends to occur in class 2 and class 3 of obesity [11]. Consequently, the PMHS used for comparison here (BMI 35 and 45 kg/m^2), are representative of occupants with an increased risk of mortality in automobile collisions due to obesity.

The only other currently available large male dummy is the Hybrid III 95th percentile male. At 188 cm in height and 101 kg in mass, the Hybrid III 95th represents a BMI of 28.6 kg/m^2. This is less than the 70th percentile US adult male BMI. The Hybrid III 95th also does not take into account changes in body mass distribution or increases in superficial soft tissue depth associated with obesity. Similar to the Hybrid 95th percentile male the FGOA represents an extreme proportion of the population, but does so in a manner that more accurately replicates the changes in body habitus and soft tissue distribution that occurs with obesity.

Obesity can result in a wide variety of body mass distribution and anthropometry characteristics, complicating efforts to develop and evaluate an "average" obese occupant model. To facilitate a direct biofidelity assessment, the anthropometry of this dummy prototype was developed based on a specific PMHS for which sled testing data was available. Thus, this may be considered as an effort to evaluate the general design methods and materials used for the obese dummy retrofit. If the design of this dummy retrofit can be validated against a specific matching PMHS, then the anthropometry of the retrofit may later be modified to represent a different target obese anthropometry for which sled testing data may not be available. Such a modification could be made based on body mass distribution targets from the more general obese population. Any effort to quantify an "average" obese anthropometry should include a consideration for characteristic anthropometry patterns using methods such as Principal Component Analysis or similar.

The study was limited to using PMHS tests already existing in the literature. As a result, the standing stature of the target PMHS was somewhat greater than the standing stature of the FGOA. Despite this difference, the interaction with the restraint systems is likely more dependent on the seated anthropometry. As can be seen in Figure 2 and Table II, the FGOA and PMHS #404 exhibited a similar seated head-to-buttock height measurement (within 5%, compared to an 11% difference in stature) and similar initial shoulder heights. Thus, the geometry relative to the restraint systems is more similar than it would appear if one were to consider stature alone. Similarly, although the body region dimensions were designed targeting those of PMHS #404, due to manufacturing limitations some differences were bound to occur. For example, that PMHS carried a disproportionate amount of his upper body mass in his lower chest and abdomen (as can be seen in the abdominal protuberance shown in Figure 2). In achieving the target abdominal dimensions, however, the dummy exhibited a somewhat greater upper chest depth and circumference compared to the PMHS. When such competing design and manufacturing factors are present, a balance is required considering the likely effects of each parameter. In this case, it was hypothesized that the abdominal dimensions would have a greater effect on the overall kinematics due to the interaction with the lap belt. Further refinement of the FGOA may include investigating the effects of the upper chest dimensions, and revising the upper chest anthropometry if needed.

Repeatability of the FGOA

Though only two tests were performed in each condition, the FGOA exhibited a reasonable repeatability between these tests. For example, the average coefficient of variation (CV) for the head acceleration time history was 0.09 and 0.07 in the FGOA 29 and 48 km/h tests, respectively. In addition, CV of the head, shoulder, pelvis and knee maximum forward motion was 0.02, 0.02, 0.02 and 0.07, respectively, in the FGOA 48 km/h tests. Similarly, average CV for the FGOA's torso angle time history was 0.01 and 0.02 in 29 and 48 km/h tests, respectively. While this is encouraging, additional study on the effects of increased dummy soft tissue on repeatability, reproducibility, and durability may be warranted.

Kinematic Comparison

In the 29 km/h tests, the FGOA exhibited similar forward head excursion and shoulder excursion compared to the PMHS, and somewhat greater forward motion of the pelvis and knee (roughly 26% greater). Similar trends were seen in the 48 km/h tests, with somewhat greater forward motion of the pelvis and knee with the dummy compared to the PMHS.

Forman et al. [15] and Kent et al. [14] previously observed that one of the critical kinematic differences observed between obese subjects and mid-sized subjects was the nature of the rotation of the upper body throughout the interaction with the restraints. Due to increased forward excursion of the pelvis, the upper body tended to exhibit very little forward rotation of the torso with the obese PMHS, compared to greater forward rotation of the torso with the mid-sized PMHS. In other words, with the obese PMHS the entire body tended to move forward into the restraint system, with very little torso rotation. This phenomenon was replicated with the FGOA (Fig. 7).

The isolated spikes in head acceleration and pelvis acceleration observed with the FGOA can, for the most part, be attributed to various acute kinematic phenomena. In the 48 km/h dummy tests, the FGOA's head rotated downward towards chest and hit left arm, causing an acute spike in head acceleration. This may be attributable to the FGOA's lack of flesh around the exterior of the neck, which may allow increased forward flexion. If this spike is discounted, then the FGOA and PMHS exhibited similar peak head acceleration. The FGOA and PMHS also exhibited similar peak head accelerations in the 29 km/h tests. Nevertheless, the acceleration behavior after the peak and maximum head angular velocity were different between the two groups of surrogates. This may be the result of greater stiffness in the FGOA's neck, which is designed to include the effects of active musculature. The stiffness of the PMHS neck is very non-linear, having very little stiffness over most of its range of motion with a dramatic increase in stiffness at the end of its range of motion. In contrast, the greater stiffness of the FGOA neck over its entire range of motion may tend to increase the duration of the head acceleration pulse as shown in Figure 8. Even with this, however, the head acceleration of both surrogate groups is affected by the motions and interactions of the other body regions, rendering it difficult to identify a single underlying cause for any differences or similarities.

The FGOA also exhibited an acute spike in pelvis acceleration in the 48 km/h tests, occurring when the dummy's pelvis travelled off the front edge of the seat and moved down into the floorpan. Such a spike can also be observed in PMHS test 1335, where the PMHS also travelled off the seat and into the floorpan. If these spikes are discounted, then the FGOA and PMHS exhibited similar general patterns of pelvis acceleration, with the PMHS exhibiting a greater high-frequency content of pelvis acceleration, presumably due to differences in compliance in the pelvis and lumbar spine. The FGOA and PMHS also exhibited similar chest accelerations, with the FGOA peak chest accelerations falling within 10% of the PMHS.

A limitation for the kinematic analysis was that as the photo targets were externally mounted, and thus could potentially move relative to the underlying skeletal structure. Since the FGOA's exterior is intended to mimic the stiffness of flesh, the potential error induced by flesh motion is expected to be comparable between two groups of surrogates. A more detailed kinematic comparison may require additional PMHS tests performed with 3D motion capture to track the motion of specific skeletal landmarks (e.g. [22-23]).

Restraint System

Peak lower and upper shoulder-belt forces were similar between the FGOA and PMHS, especially in the 48 km/h tests. The lap-belt forces, however, were greater with the FGOA compared to the PMHS (64% greater in the 29 km/h tests and 18% greater in the 48 km/h tests). This, combined with the greater forward motion of the pelvis and lower extremities exhibited by the FGOA, suggests that the FGOA interacted with the seat/seat cushion in a manner that was different from the PMHS. The PMHS tended to tear the seat cushion off the seatpan in the 48 km/h tests, causing substantial deformation and/or failure of the metallic clips that secure the seat cushion to the seatpan. In contrast, the FGOA tended to slide over the seat cushion, resulting in less deformation of the seat cushion attachment hardware. This suggests that in the PMHS tests, a greater portion of the restraining load was provided by interaction with the seat cushion, helping off-load the lap-belt and limit forward pelvis excursion. Thus, future refinement of the FGOA should include consideration for the interaction with the seat cushion, including modifications to increase engagement with the seat cushion.

Perhaps most importantly, the obese ATD exhibited the kinematic characteristics that have previously been highlighted as potentially challenging for occupant restraint. Particularly, the addition of soft tissue material to the lower body limited the engagement of the pelvis in a manner similar to that observed with the obese PMHS. This, combined with increased body mass, resulted in a substantially greater (more than two times) forward motion of the lower body, with limited torso rotation, compared to what would be expected of a mid-sized dummy or PMHS [14-15]. This increased forward motion of the lower extremities may contribute to lower extremity injury risk [12] through interaction with other vehicle structures (e.g. knee bolsters, toe pans, intruding structures). Penetration of the lap-belt into the abdomen may also affect abdominal organ injury risk [24].

Though further refinement and evaluation may be warranted, the general challenges replicated by this dummy may provide a preliminary tool for designers to develop and evaluate new concepts for improved restraint for obese occupants. Given the diversity of anthropometries present in the field, such physical evaluations may be augmented through morphed human body computer modelling parametrically sweeping a range of occupant characteristics.

V. CONCLUSIONS

A preliminary biofidelity evaluation was performed with a first generation obese ATD compared to two obese PMHS in frontal impact sled tests. The FGOA and PMHS exhibited similar head and upper body kinematics (excursions and accelerations), and both exhibited lower body kinematics that demonstrate the challenges posed to restraint system design. The FGOA exhibited somewhat greater concomitant pelvis motion and lap belt force, suggesting differences in the interaction with the seat/seat cushion. Though further refinement may be warranted, this dummy may provide a useful preliminary tool for designers to develop and evaluate new concepts for improved restraint for obese occupants.

VI. ACKNOWLEDGMENTS

The obese ATD was developed and provided by Humanetics Innovative Solutions Corporation. The sled buck was provided by Ford Motor Corporation. The authors would also like to acknowledge the assistance and support of the students and staff of the UVA Center for Applied Biomechanics.

VII. REFERENCES

[1] World Health Organization. Physical status: the use and interpretation of anthropometry, Geneva, Switzerland, 1995.

[2] Li, C., Ford, E. S., McGuire, L. C., Mokdad, A. H. Increasing trends in waist circumference and abdominal obesity among U.S. adults. *Obesity,* January 2007, Vol. 15(1):216–24.

[3] Ladabaum, U.,, Mannalithara, A., Myer, P. A., Singh, G. Obesity, abdominal obesity, physical activity, and caloric intake in US adults: 1988 to 2010. *The American Journal of Medicine*, 2014, Volume 127(8):717–27.

[4] Ogden, C. L., Carroll, M. D., Kit, B. K., Flegal, K. M. Prevalence of obesity in the United States, 2009–2010. NCHS Data Brief, No. 82, January 2012.

[5] Ogden, C. L., Carroll, M. D., Kit, B. K., Flegal, K. M. Prevalence of childhood and adult obesity in the United States, 2011-2012. *JAMA*, Feb. 2014, Vol. 311:806–14.

[6] Choban, P. S., Weireter, L. J., Maynes, C. Obesity and increased mortality in blunt trauma. *Journal of Trauma,* Setember 1991, Vol. 31(9):1253–7.

[7] Neville, A. L., Brown, C. V., Weng, J., Demetriades, D., Velhamos, G. C. Obesity is an independent risk factor of mortality in severely injured blunt trauma patients. *Arch. Surg*. September 2004, Vol. 139:983–7.

[8] Zhu, S., Layde, P. M., et al. Obesity and risk for death due to motor vehicle crashes. *American Journal of Public Health*, April 2006, Vol, 96(4):734–9.

[9] Mock, C. N., Grossman, D. C., Kaufman, R. P., Mack, C. D., Rivara, F. P. The relationship between body weight and risk of death and serious injury in motor vehicle crashes. *Accid Anal Prev,* March 2002, Vol. 34:221–8.

[10] Jehle, D., Gemme, S., Jehle, C. Influence of obesity on mortality of drivers in severe motor vehicle crashes. *The American Journal of Emergency Medicine*, January 2012, Volume 30:191–5.

[11] Rice, T. M., Zhu, M. Driver obesity and the risk of fatal injury during traffic collisions. *Emerg Med J*, January 2014, Vol. 31:9–12.

[12] Arbabi, S., Wahl, W. L., et al. The cushion effect. *J Trauma*, 2003, Vol. 54:1090–93.

[13] Cormier, J. M. The influence of body mass index on thoracic injuries in frontal impacts. *Accident Analysis & Prevention*, March 2008, Volume 40:610–15.

[14] Kent, R., Forman, J., Bostrom, O. Is there really a "cushion effect"?: a biomechanical investigation of crash injury mechanisms in the obese. *Obesity*, April 2010, Vol. 18:749–53.

[15] Forman, J., Lopez-Valdes, F. J., Lessley, D., Kinding, M., Kent, R. The effect of obesity on the restraint of automobile occupants. *AAAM*, 2009, Vol. 53:25–40.

[16] Reed, M. P., Ebert, S. M., Hallman, J. J. Effects of driver characteristics on seat belt fit. *Stapp Car Crash Journal*, November 2013, Vol. 57:43–57.

[17] Forman, J., Michaelson, J., Kent, R., Kuppa, S., Bostrom, O. Occupant restraint in the rear seat: ATD responses to standard and pre-tensioning, force-limiting belt restraints. *Ann Adv Automot Med.*, 2008, Vol. 52:141–54.

[18] Flegal, K. M., Carroll, M. D., Kit, B. K., Ogden, C. L. Prevalence of obesity and in the distribution of body mass index among US adults, 1999-2010. *JAMA*, 2012, Vol. 307(5):491–7.

[19] Hedrick, T. L. Software techniques for two and three-dimensional kinematic measurements of biological and biomimetic systems. *Bioinspiration and Biomimetics*, 2008, Vol. 3.

[20] Shaw, G., Crandall, J., Butcher, J. Comparative evaluation of the THOR advanced frontal crash test dummy. *International Journal of Crashworthiness*, 2002, Vol. 7(3).

[21] World Health Organization. Obesity: Preventing and managing the global epidemic. Report of a WHO consultation of obesity, Geneva, Switzerland, 3–5 June 1997. *J. Biosens. Bioelectronics*, 2011, S1.

[22] Lessley, D., Shaw, G., Riley, P., Forman, J., Crandall, J. Assessment and validation of a methodology for measuring anatomical kinematics of restrained occupants during motor vehicle collisions.

[23] Shaw, G., Parent, D., Purtsezov, S., Lessley, D., Crandall, J., Kent, R. Impact response of restrained PMHS in frontal sled tests: skeletal deformation patterns under seat belt loading. *Stapp Car Crash Journal*, 2009, Vol. 53:1-48.

[24] Poplin, G., McMurry, T., et al. Nature and etiology of hollow-organ abdominal injuries in frontal crashes. *Accid Anal Prev*. 2015:51–7.